

## miR-182-5p Induced by STAT3 Activation Promotes Glioma Tumorigenesis

Jianfei Xue<sup>1</sup>, Aidong Zhou<sup>1</sup>, Yamei Wu<sup>2</sup>, Saint-Aaron Morris<sup>1</sup>, Kangyu Lin<sup>1</sup>, Samirkumar Amin<sup>3</sup>, Roeland Verhaak<sup>3</sup>, Gregory Fuller<sup>4</sup>, Keping Xie<sup>5,6</sup>, Amy B. Heimberger<sup>1</sup>, and Suyun Huang<sup>1,6</sup>

### Abstract

Malignant glioma is an often fatal type of cancer. Aberrant activation of STAT3 leads to glioma tumorigenesis. STAT3-induced transcription of protein-coding genes has been extensively studied; however, little is known about STAT3-regulated miRNA gene transcription in glioma tumorigenesis. In this study, we found that abnormal activation or decreased expression of STAT3 promotes or inhibits the expression of miR-182-5p, respectively. Bioinformatics analyses determined that tumor suppressor protocadherin-8 (PCDH8) is a candidate target gene of miR-182-5p. miR-182-5p negatively regulated PCDH8 expression by directly targeting its 3'-untranslated

region. PCDH8 knockdown induced the proliferative and invasive capacities of glioma cells. Silencing of PCDH8 or miR-182-5p mimics could reverse the inhibitory effect of WP1066, a STAT3 inhibitor, or STAT3 knockdown *in vitro* and *in vivo* on glioma progression. Clinically, expression levels of PCDH8 were inversely correlated with those of p-STAT3 or miR-182-5p in glioblastoma tissues. These findings reveal that the STAT3/miR-182-5p/PCDH8 axis has a critical role in glioma tumorigenesis and that targeting the axis may provide a new therapeutic approach for human glioma. *Cancer Res*; 76(14); 4293–304. ©2016 AACR.

### Introduction

Glioma is one of the most common types of primary brain tumor in humans. Glioblastoma is the highest grade and most aggressive malignant glioma (1). A major feature of malignant glioma is its diffuse infiltrative growth into surrounding brain tissue (2). The oncogenic transcription factor STAT3, a component of the Janus-activated kinase (JAK)/STAT3 signaling pathway, plays a key role in many physiologic and pathophysiologic processes including cancer growth, invasion, and metastasis (3–5). STAT3 is mainly activated via tyrosine phosphorylation (Tyr705) by growth factor/cytokine receptors and non-receptor tyrosine kinases, which results in STAT3 nuclear

translocation and thus subsequent activation of various STAT3 target genes that regulate cell proliferation, migration, and invasion (6, 7). In glioma, activation of STAT3 often positively correlates with tumor malignancy and indicates poor prognosis (8–10).

miRNAs are a class of evolutionally conserved small, noncoding RNA molecules (~19–23 nucleotides) that are involved in posttranscriptional regulation of gene expression in animals, plants, and viruses (11, 12). The alteration in miRNA expression profiles represents a common feature in all human cancers, indicating the importance of such alterations in cancer progression and prognosis (13). miR-182-5p is a well-described oncomiR that is overexpressed in a number of malignancies including glioma (14), lung (15), breast (16), prostate (17), liver (18), and colorectal (19) cancers. Given the importance of both miR-182-5p and STAT3 in the processes linked to cancer, we sought to test whether both may be part of a common pathway. Moreover, STAT3-induced transcription of protein-coding genes has been extensively studied; however, little is known about STAT3-regulated miRNA gene transcription.

In this study, we present evidence that STAT3-induced miR-182-5p promotes glioma cell growth, migration, and invasion by suppressing PCDH8 (protocadherin 8). In addition, the STAT3–miR-182-5p–PCDH8 axis is critical for glioma tumor growth *in vivo*. We found that expression of both p-STAT3 and miR-182-5p is upregulated in glioblastoma compared with their expression in normal brain tissues; however, expression of PCDH8 is higher in normal brain tissues than in tumor tissues. The expression levels of PCDH8 are inversely correlated with those of p-STAT3 or miR-182-5p in glioblastoma tissues. Therefore, our data shed light on the molecular mechanisms of the growth- and invasion-promoting function of the axis and suggested that the axis may include potential prognostic markers and therapeutic targets.

<sup>1</sup>Department of Neurosurgery, The University of Texas MD Anderson Cancer Center, Houston, Texas. <sup>2</sup>Department of Hematology, The First Affiliated Hospital, Chinese PLA General Hospital, Beijing, China. <sup>3</sup>Department of Genomic Medicine; Department of Bioinformatics and Computational Biology, The University of Texas MD Anderson Cancer Center, Houston, Texas. <sup>4</sup>Department of Pathology, The University of Texas MD Anderson Cancer Center, Houston, Texas. <sup>5</sup>Department of Gastroenterology, Hepatology & Nutrition, The University of Texas MD Anderson Cancer Center, Houston, Texas. <sup>6</sup>Program in Cancer Biology, The University of Texas Graduate School of Biomedical Sciences at Houston, Houston, Texas.

**Note:** Supplementary data for this article are available at Cancer Research Online (<http://cancerres.aacrjournals.org/>).

J. Xue, A. Zhou, and Y. Wu contributed equally to this article.

**Corresponding Author:** S. Huang, Department of Neurosurgery, The University of Texas MD Anderson Cancer Center, Unit 1004, 1515 Holcombe Blvd., Houston, TX 77030. Phone: 713-834-6232; Fax: 713-834-6257; E-mail: suhuang@mdanderson.org

**doi:** 10.1158/0008-5472.CAN-15-3073

©2016 American Association for Cancer Research.

## Materials and Methods

### Plasmids, siRNAs, reagents, and antibodies

The expression vector encoding STAT3 CA was obtained from Addgene (Plasmid #24983). SMARTpool siRNA duplexes specific for STAT3, PCDH8, and a nontargeting siRNA (siControl) were purchased from Dharmacon. Recombinant human EGF was purchased from R&D Systems. miR-182-5p mimics and inhibitor were obtained from Sigma-Aldrich. WP1066 was synthesized at The University of Texas MD Anderson Cancer Center (Houston, TX). STAT3 (#4904) and p-STAT3 (#9131) were purchased from Cell Signaling Technology. PCDH8 (#ab55507) was purchased from Abcam.  $\beta$ -Actin (#sc-47778) was purchased from Santa Cruz Biotechnology.

### Cell culture and transfection

HEK 293T cells and the human glioma cell lines SW1783, Hs683, LN229, and U87 were purchased from ATCC between years 2009 and 2015. The HFU251 human glioma cell line was obtained from our brain tumor center core and was described previously (20). The cell lines were subjected to cell line characterization and authentication using short tandem repeat profiling in every 6 months, and the cells were passaged continuously for fewer than 6 months after receipt in our laboratory for relevant studies reported here. All of the cell lines were grown in DMEM containing 10% FBS (HyClone).

HEK 293T cells were transfected with FuGENE HD (Roche). SW1783, Hs683, HFU251, and U87 cells were transfected with X-tremeGENE HP (Roche). SW1783 and U87 cells were transfected with siRNA using Lipofectamine RNAiMAX (Invitrogen).

### Lentiviral generation and infection

For STAT3 or PCDH8 silencing of expression, lentiviral particles were produced with use of a lentivirus packaging mix (ViraPower, Invitrogen). For viral transduction, the cells were seeded at 50%–60% confluence. The cells were treated overnight, with the medium containing lentivirus harvested 48 or 72 hours after transfection. Virus particles were concentrated and purified by ultra-high-speed centrifugation ( $25,000 \times g$  for 2 hours at  $4^\circ\text{C}$ ). Puromycin or hygromycin (Sigma-Aldrich) was used to select stable clones.

### Western blot analysis

Cells were lysed with RIPA lysis buffer; cell lysates were then subjected to an 8%–12% SDS-PAGE, transferred onto polyvinylidene difluoride membrane, and probed with antibodies, as previously described (21).

### Luciferase promoter assay and 3'-UTR luciferase reporter

The miR-182-5p promoter was produced by PCR by using primers 5'-TTTACGCGTGTGTTGTTGAGACAGAATCTCGCT-3' (forward) and 5'-TTTAAGCTCCTGCCGACCCTGCCGAGAGA-3' (reverse). In the promoter assay, SW1783 cells were transfected with pGL3-miR-182-5p, STAT3 CA plasmid, and *Renilla*. The wild-type (WT) and mutant 3'-UTRs luciferase reporter of the *pcdh8* gene were generated by annealing the forward and reverse oligonucleotides and were then cloned into psi-Check2 vector. Oligonucleotides for the *pcdh8* 3'-UTR were as follows: WT, 5'-TCGAGATAATAAAAGCTAAAGT-GGAAGTTATTGCCAAAGGAACTGTCTGTAGC-3' (forward) and 5'-GGCCGCTACAGACAGTTCCTTTGGCAATAACTTCCAC-TTAGCTTTTATTATC-3' (reverse); mutant, 5'-TCGAGATAAT

AAAAGCTAAAGTGGAAAGTTATGGACCAAGGAACTGTCTGTAG-CC-3' (forward) and 5'-GGCCGCTACAGACAGTTCCTTGG-TCCATAACTTCCACTTTAGCTTTTATTATC-3' (reverse). In the 3'-UTR reporter assay, HEK 293T cells were transfected with the psi-Check2-PCDH8 3'-UTR (WT or mutant), *Renilla*, together with miR-182-5p mimics/inhibitor or with control mimics/inhibitor. Luciferase activity was measured in a 1.5-mL Eppendorf tube with the Promega Dual-Luciferases Reporter Assay Kit (Promega E1980) according to the manufacturer's protocols after transfection. Relative *Renilla* luciferase activity was normalized to firefly luciferase activity.

### Quantitative real-time RT-PCR

Total RNA was extracted with use of TRIzol reagent (Invitrogen) for miR-182-5p or PCDH8 mRNA analyses. For detection of miR-182-5p expression, stem-loop RT-PCR was performed. Quantitative real-time RT-PCR was performed by using the SYBR green reagent with an ABI Prism 7000HT sequence detection system. Relative expression was evaluated by a comparative  $C_T$  method and normalized to the expression of U6 small RNA or *GAPDH*. The stem loop primer for miR-182-5p is 5'-GTCGTATCCAGTGCAGGGTCCGAGGATATTCGACTGG-ATACGACAGTGTG-3'. The qPCR primer for miR-182-5p was purchased from Sigma.

### Chromatin immunoprecipitation assay

U87 or LN229 cells ( $2 \times 10^6$ ) were prepared for the chromatin immunoprecipitation (ChIP) assay by using a ChIP Assay Kit (Cell Signaling Technology) according to the manufacturer's protocol. The resulting precipitated DNA specimens were analyzed by using PCR to amplify a 298-bp region (site 1) of the miR-182-5p promoter with the primers 5'-GGTTTCACCATGCTAACCAGGCT-3' (forward) and 5'-TAGCCATAAGCATCACCCAAGGAG-3' (reverse) and a 300-bp region (site 2) of the miR-182-5p promoter with the primers 5'-GGCTCAAGAATCTACATTTCAACAG-3' (forward) and 5'-ACACCCCCACTACAGGGCTCT-3' (reverse). The negative control is an encoding region of miR-182-5p, which was amplified by PCR with the primers 5'-ATAGTTGGCAAGTCTAGAAC-3' (forward) and 5'-TCTGTCTCTTCTCAGCACA-3' (reverse). The PCR products were resolved electrophoretically on a 2% agarose gel and visualized with use of ethidium bromide staining.

### Cell proliferation assay

For the cell proliferation assay,  $5 \times 10^3$  cells were plated in 96-well plates. Cell growth was determined by using a standard tetrazolium bromide (MTT) assay and verified by counting with trypan blue and a hemocytometer. Data represent the means  $\pm$  SD of 3 independent experiments.

### Transwell migration and invasion assays

After transfection, SW1783 or U87 cells ( $5 \times 10^4$ ) in a 500- $\mu\text{L}$  volume of serum-free medium were placed in the upper chambers of a Transwell and incubated at  $37^\circ\text{C}$  for 16 hours for the migration or invasion assay. The cells that penetrated the uncoated (migration) or Matrigel-coated (invasion) filters were counted at a magnification of  $\times 200$  in 15 randomly selected fields, and the mean number of cells per field was recorded.

### Intracranial injection

All mouse experiments were approved by the Institutional Animal Care and Use Committee of The University of Texas MD

Anderson Cancer Center. We intracranially injected glioblastoma stable cells into 4-week-old female athymic nude mice. Five mice were injected for each group. Mice were euthanized 4 weeks after the glioblastoma cell injection. The brain of each mouse was harvested, fixed in 4% formaldehyde, and embedded in paraffin. Tumor formation and phenotype were determined by histologic analysis of hematoxylin and eosin (H&E)-stained sections.

#### Human or mouse tissue samples and immunohistochemical analysis

Human or mouse normal brain and brain tumor tissues were stored frozen at  $-75^{\circ}\text{C}$  until use for qPCR analysis. For immunohistochemical (IHC) analysis, mouse tumor tissues were fixed and prepared for staining. The specimens were stained with Mayer's hematoxylin and subsequently with eosin (Biogenex Laboratories) or with antibodies against p-STAT3 and PCDH8. The tissue sections from paraffin-embedded human glioblastoma specimens were stained with antibodies against p-STAT3 and PCDH8. IHC analyses were performed on the tissue arrays by a standard immunostaining protocol (22). The use of human brain tumor specimens was approved by the Institutional Review Board at The University of Texas MD Anderson Cancer Center and written informed consent was obtained from the patients for the use of clinical specimens for research.

#### Statistical analysis

The significance of the data from patient specimens was determined by the Pearson correlation coefficient test. The significance of the *in vitro* data and *in vivo* data between experimental groups was determined by Student *t* test or Mann-Whitney U-test.  $P < 0.05$  was considered to be statistically significant.

## Results

### STAT3 activation upregulates miR-182-5p expression

To ascertain the role of miR-182-5p in glioma tumorigenesis, we first determined that miR-182-5p expression by quantitative real-time RT-PCR analysis was significantly increased in human glioblastoma tissues compared with its expression in normal human brain tissues (Fig. 1A). Quantitative real-time RT-PCR analysis revealed that miR-182-5p expression was markedly increased in a panel of glioma cell lines tested (Hs683, SW1783, HFU251, and U87), compared with its expression in normal human astrocytic cells. Among the glioma cell lines, miR-182-5p showed lower expression in the grade III-derived glioma cell lines (Hs683 and SW1783) relative to the glioblastoma grade IV cell lines (HFU251 and U87; Fig. 1B). Furthermore, we found that the glioblastoma cell lines expressed higher levels of activated STAT3 (p-STAT3) than the grade III glioma cell lines (Fig. 1C), suggesting the levels of miR-182-5p directly correlated with the expression of activated STAT3. When the SW1783 cells were transfected with a constitutively activated mutant of STAT3 (STAT3 CA), miR-182-5p was increased (Fig. 1D). In addition, when the SW1783 cells were treated with a ligand for STAT3 activation, EGF, miR-182-5p was upregulated (Fig. 1E), suggesting that STAT3 activation positively regulates miR-182-5p expression. In contrast, inhibition of STAT3 by siRNA or WP1066 (23–25), a STAT3 inhibitor, strongly reduced miR-182-5p expression levels in U87 cells (Fig. 1F and G).

Next, we analyzed the sequence of the miR-182-5p promoter by using the STAT3 consensus sequences AA (N4) TT and AA (N5) TT. We identified 2 putative STAT3-binding sites in the miR-182-5p promoter (sites 1 and 2, Fig. 1H). To provide direct evidence that miR-182-5p is a direct transcriptional target of STAT3, we performed standard ChIP assays in glioma cells using primers that flank a 298-bp region (containing STAT3 binding site 1) or a 300-bp region (containing STAT3 binding site 2) of the miR-182-5p promoter. We found that in U87 cells, endogenous STAT3 protein bound to both of the STAT3-binding regions of the miR-182-5p promoter, but not to an miRNA-encoding region (MER) of miR-182-5p (Fig. 1H). Similar results were detected in LN229 cells (Fig. 1H). Moreover, knocking down STAT3 by siRNA in U87 cells reduced the binding of miR-182-5p promoter to STAT3 protein (Supplementary Fig. S1). These findings indicated that STAT3 protein directly interacts with the miR-182-5p promoter. To provide further evidence that miR-182-5p is a direct transcriptional target of STAT3, we examined whether STAT3 activation transactivates the miR-182-5p promoter by using a miR-182-5p promoter luciferase reporter with the STAT3 CA or the control vector. Luciferase activity driven by the miR-182-5p promoter increased in SW1783 cells overexpressing STAT3 CA (Fig. 1I). These results suggested that STAT3 is involved in miR-182-5p transcriptional activation.

### miR-182-5p promotes glioma cell growth, migration, and invasion

To determine whether miR-182-5p promotes an oncogenic phenotype of glioma, we performed overexpression or knock-down function assays in glioma cells by using an miR-182-5p mimics or inhibitor. Overexpression of miR-182-5p resulted in a significant increase in viability in Hs683 and SW1783 cells in an MTT assay (Fig. 2A). In contrast, as shown in Fig. 2B, miR-182-5p inhibition significantly reduced glioma cell growth compared with the scramble control cells in HFU251 and U87 cells, as measured by an MTT assay.

Furthermore, we performed Transwell migration and invasion assays to determine whether miR-182-5p regulates glioma cell migration and invasion abilities. We found that miR-182-5p increased the ability of SW1783 cells to migrate and invade (Fig. 2C). In contrast, miR-182-5p inhibition significantly reduced U87 cells migration and invasion abilities (Fig. 2D).

### miR-182-5p directly targets PCDH8 3'-UTR

To identify the miR-182-5p-mediated downstream regulator, 3 target prediction algorithms (PicTar, TargetScan, and miRanda) were used. We analyzed first 100 picks from each of the three algorithms and found that 5 genes are overlapped, namely, ARF4, CTTN, EDNRB, PCDH8, and RASA1 (Fig. 3A). To determine whether miR-182-5p targets these genes, we generated luciferase reporter plasmids that harbor miR-182-5p target sequences in 3'-UTR (untranslated repeat) of these genes. By using these luciferase reporter plasmids, we found that miR-182-5p mimics did not significantly inhibit the activities of 3'-UTR luciferase reporters of ARF4, CTTN, EDNRB, or RASA1 gene (Supplementary Fig. S2). However, expression of miR-182-5p mimics caused a strong inhibition in the activities of 3'-UTR luciferase reporter of PCDH8 gene (Supplementary Fig. S2). Indeed, PCDH8 contains miR-182-5p target and seed motifs, located in the 3'-UTR (Fig. 3B). It has been

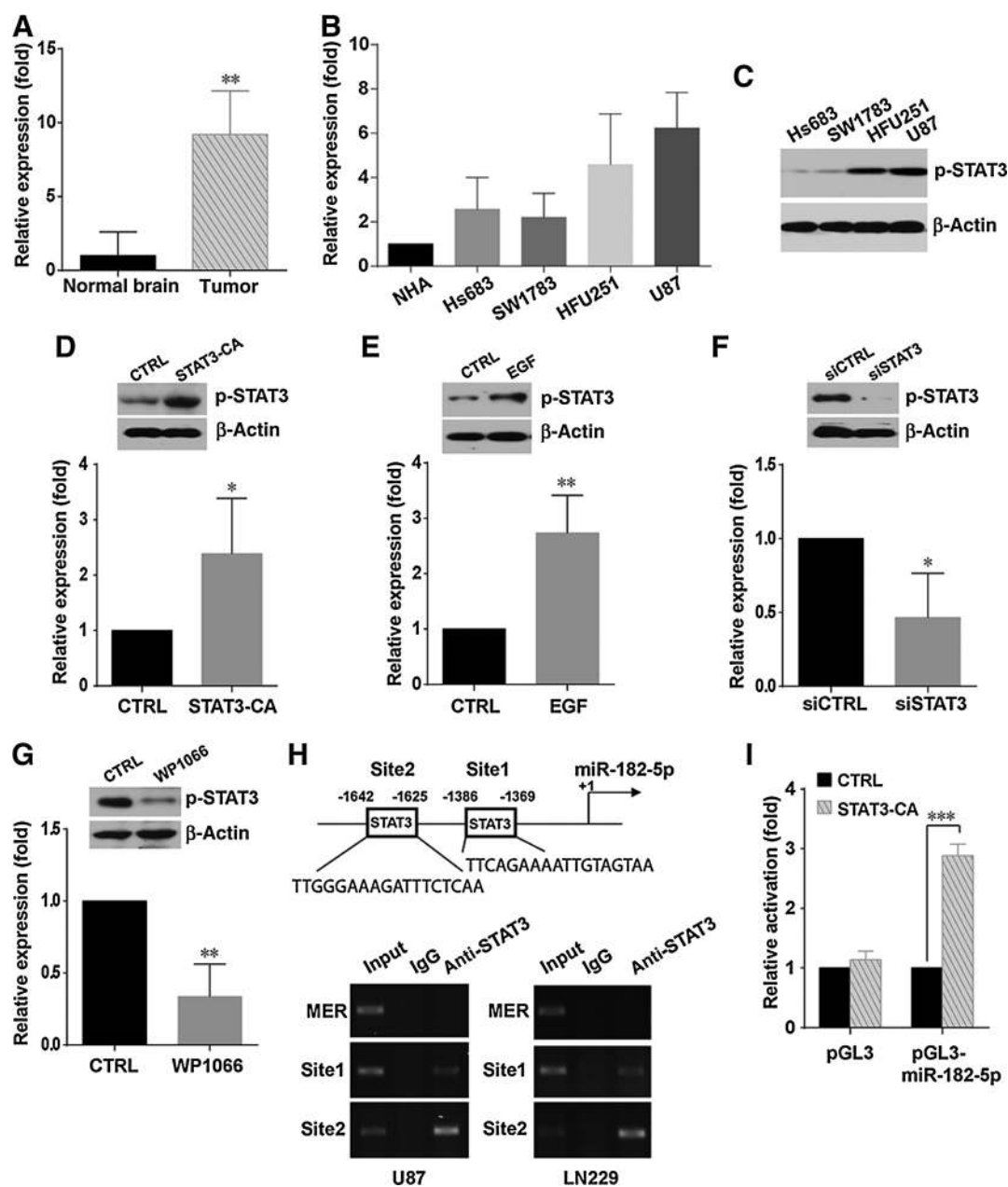


**Figure 1.**

STAT3 activation upregulates miR-182-5p expression. A, relative ratios of miR-182-5p expression in 20 glioblastoma tissues compared with 10 normal brain tissues. \*\*,  $P < 0.01$ . B, histograms of the average relative expression of miR-182-5p in a normal human astrocytic (NHA) cell line and glioma cell lines (Hs683, SW1783, HFU251, and U87). Data are presented as mean  $\pm$  SD from three independent experiments. C, protein level of p-STAT3 was determined by Western blot analyses in glioma cell lines (Hs683, SW1783, HFU251, and U87). D, levels of miR-182-5p expression in SW1783 cells after transfection with a constitutively activated mutant of STAT3 (STAT3 CA) and empty vector (control). p-STAT3 level was determined by Western blot analyses. Data are means  $\pm$  SD. \*,  $P < 0.05$ . E, levels of miR-182-5p expression in SW1783 cells without EGF (control) or with EGF (50 ng/mL) treatment. p-STAT3 level in 2-hour treatment was determined by Western blot analyses. Levels of miR-182-5p in 24 hours was determined by real-time RT-PCR. Data are means  $\pm$  SD. \*\*,  $P < 0.01$ . F, levels of miR-182-5p expression in U87 cells after transfection with siSTAT3 and siControl. p-STAT3 level was determined by Western blot analyses. Data are means  $\pm$  SD. \*,  $P < 0.05$ . G, levels of miR-182-5p expression in U87 cells without WP1066 (control) or with WP1066 (1.5  $\mu$ mol/L) treatment for 24 hours. p-STAT3 level was determined by Western blot analyses. Data are means  $\pm$  SD. \*\*,  $P < 0.01$ . H, top, schematic diagram indicates the location and sequences of two putative STAT3-binding sites on miR-182-5p promoter region. Bottom, ChIP assays were performed in U87 and LN229 cells with anti-STAT3 antibody and primers for miR-182-5p promoter described in Materials and Methods. Primers for an MER were used as a negative control. I, empty vector or STAT3 CA plasmid were cotransfected with pGL3 or pGL3-miR-182-5p plasmids into SW1783 cells for 36 hours and then cells were harvested for luciferase activity assays. Each error bar indicates the variation between the means of three independent experiments. \*\*\*,  $P < 0.001$ .

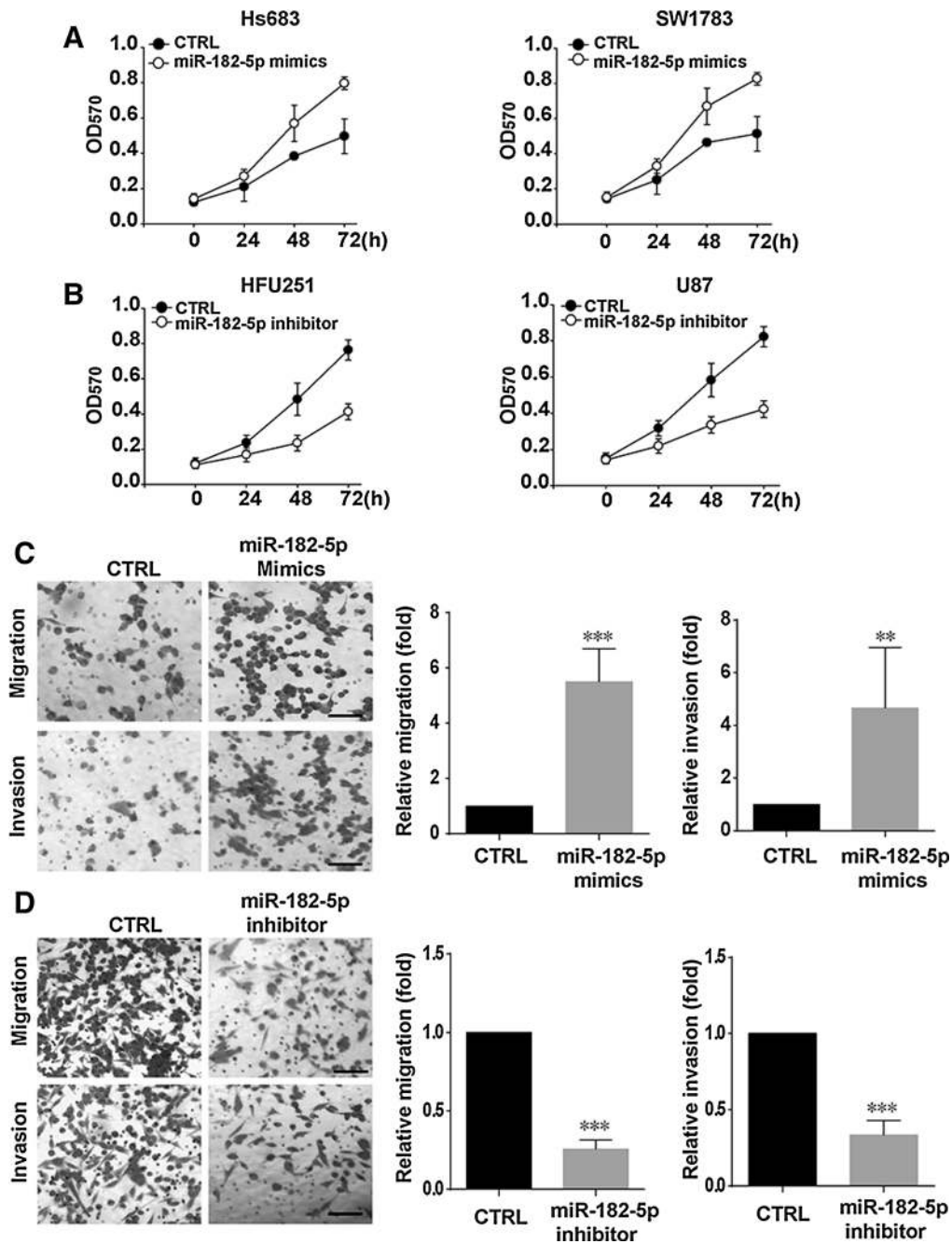


**Figure 2.**

miR-182-5p promotes glioma cell growth, migration, and invasion. A, Hs683 and SW1783 cells transfected with miR-182-5p mimics or with control mimics and their proliferation were analyzed by the MTT assay. Data are presented as mean  $\pm$  SD. B, HFU251 and U87 cells transfected with miR-182-5p inhibitor or with control inhibitor and their proliferation were analyzed by the MTT assay. Data are presented as mean  $\pm$  SD. C, SW1783 cells transfected with miR-182-5p mimics or with control mimics were subjected to Transwell migration and invasion assays. Scale bars, 100  $\mu$ m. Data are presented as mean  $\pm$  SD. \*\*,  $P < 0.01$ ; \*\*\*,  $P < 0.001$ . D, U87 cells transfected with miR-182-5p inhibitor or with control inhibitor were subjected to Transwell migration and invasion assays. Scale bars, 100  $\mu$ m. Data are presented as mean  $\pm$  SD. \*\*\*,  $P < 0.001$ .

shown that PCDH8 is a tumor suppressor in a variety of cancers, and its overexpression is associated with a better prognosis of those cancers (26). Therefore, we decided to further evaluate PCDH8 in this study. Expression of miR-182-5p in Hs683 and SW1783 cells resulted in a significant

decrease in PCDH8 protein levels (Fig. 3C), whereas inhibition of miR-182-5p in HFU251 and U87 cells resulted in increased PCDH8 protein levels (Fig. 3D). Analyses with use of 3'-UTR of luciferase reporter plasmids containing the miR-182-5p target sequences (WT or mutant) on PCDH8 were performed to

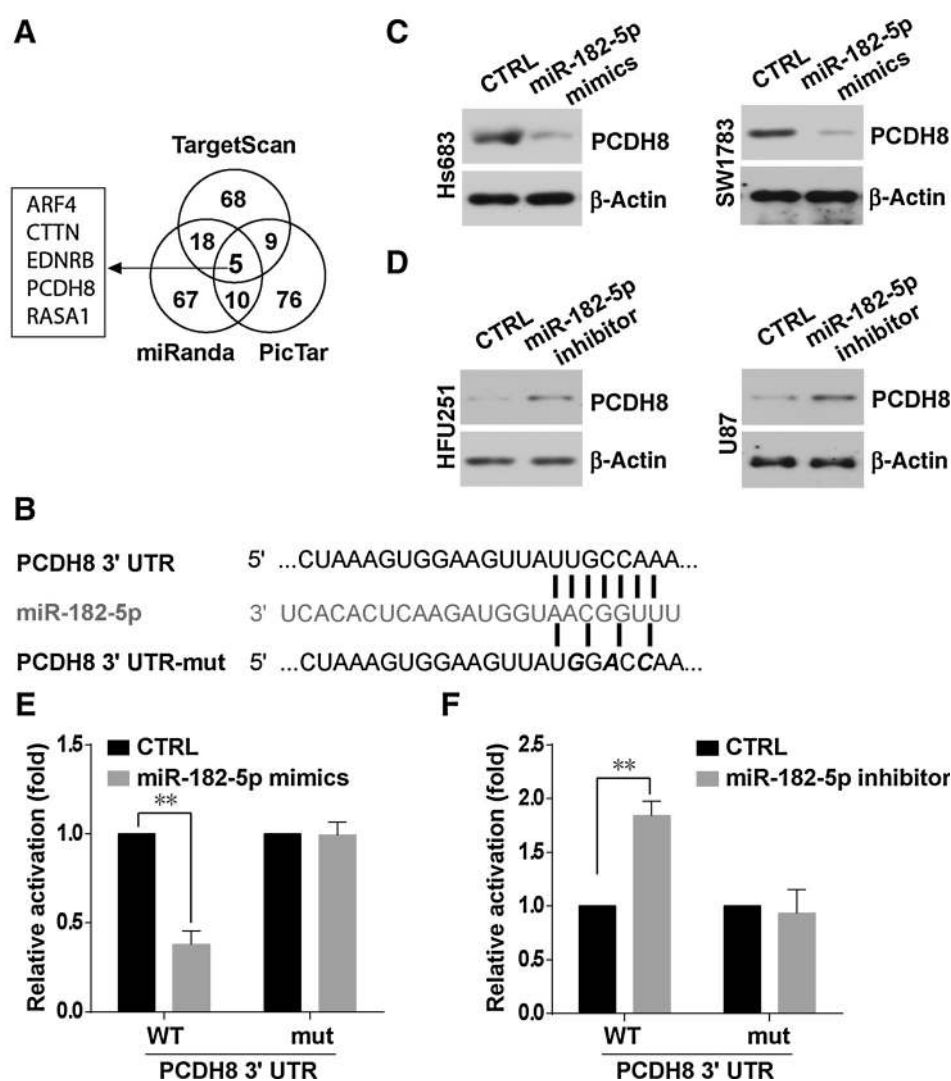


**Figure 3.** miR-182-5p directly targets *PCDH8* 3'-UTR. A, Venn diagram showing the overlap of top 100 genes potentially targeted by miR-182-5p as predicted by the following three algorithms: TargetScan, miRanda, and PicTar. B, sequence of miR-182-5p and the potential miR-182-5p-binding site at *PCDH8* 3'-UTR. Nucleotides mutated in miR-182-5p-binding site are shown in bold italic. C, protein level of *PCDH8* was determined by Western blot analyses after transfection with miR-182-5p mimics or with control mimics in Hs683 and SW1783 cells. D, protein level of *PCDH8* was determined by Western blot analyses after transfection with miR-182-5p inhibitor or with control inhibitor in HFU251 and U87 cells. E, luciferase assays demonstrating that expression of *PCDH8* 3'-UTR (WT or mutant form) by HEK 293T cells transfected with miR-182-5p mimics or with control mimics. Each error bar indicates the variation between the means of three independent experiments. \*\*,  $P < 0.01$ . F, luciferase assays demonstrating that expression of *PCDH8* 3'-UTR (WT or mutant forms) by HEK 293T cells transfected with miR-182-5p inhibitor or with control inhibitor. Each error bar indicates the variation between the means of three independent experiments. \*\*,  $P < 0.01$ .

determine whether *PCDH8* was a direct target of miR-182-5p (Fig. 3B). Expression of miR-182-5p caused a significant decrease in luciferase activity of the WT *PCDH8* 3'-UTR but not of the mutant form (Fig. 3E). In contrast, inhibition of miR-182-5p increased the luciferase activity in the WT *PCDH8* 3'-UTR but not in the mutant form (Fig. 3F). Together, these results suggest that miR-182-5p downregulates *PCDH8* expression by directly targeting its 3'-UTR.

***PCDH8* is a functional target of miR-182-5p**

To determine whether miR-182-5p can functionally target *PCDH8*, we performed rescue experiments to further demonstrate the importance of *PCDH8* in glioma cell growth, migration, and invasion by miR-182-5p. As shown in Fig. 4A, *PCDH8* expression was significantly inhibited by two different siRNAs specifically targeting *PCDH8* compared with its expression in the control in SW1783 cells. We then tested the effect of *PCDH8* knockdown in the cells. Knockdown of *PCDH8* enhanced the proliferation, migration, and invasion of SW1783 cells (Fig. 4B–D, respectively). Furthermore, we found that the downregulated miR-182-5p expression by its inhibitor signif-

icantly suppressed the proliferative, migration, and invasive capabilities of U87 cells, whereas siRNA knockdown of *PCDH8* compromised the inhibitory effect mediated by miR-182-5p (Fig. 4E–G). Thus, our data confirmed that *PCDH8* is a functional target by miR-182-5p.

**miR-182-5p/*PCDH8* is essential for STAT3-mediated glioma cell growth, migration, and invasion**

To evaluate the importance of the STAT3–miR-182-5p–*PCDH8* pathway in glioma progression, we first evaluated the consequences of targeting of STAT3 in cell growth. As anticipated, cell growth in U87 cells was significantly decreased with STAT3 knockdown or WP1066 treatment. When miR-182-5p mimics or *PCDH8* siRNA was transfected into the STAT3-inhibited U87 cells, the proliferative potential of these cells was restored (Fig. 5A and B). In addition, apoptosis in U87 and HFU251 cells significantly induced with STAT3 knockdown or WP1066 treatment, whereas the proapoptotic effect of siSTAT3 or WP1066 in these cells was inhibited by miR-182-5p mimics or *PCDH8* siRNA (Supplementary Fig. S3A and S3B). However, we found that miR-182-5p mimics or *PCDH8* siRNA alone did not affect

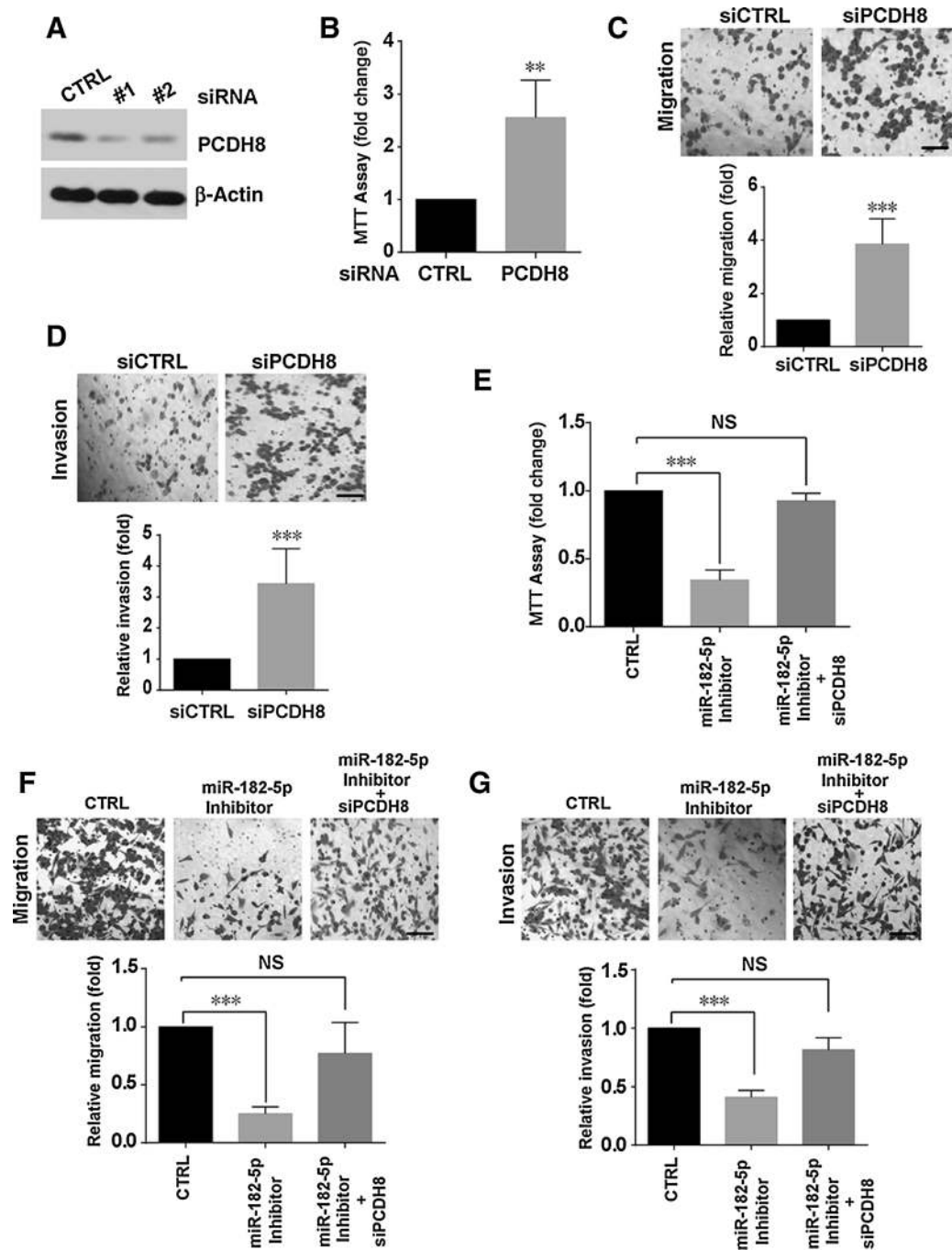


**Figure 4.**

PCDH8 is a functional target of miR-182-5p. A, PCDH8 protein level was detected by Western blot analysis after transfection with two independent PCDH8 siRNAs in SW1783 cells. B, SW1783 cells transfected with PCDH8 siRNA or with control siRNA and their proliferation were analyzed by the MTT assay. Data are presented as mean  $\pm$  SD. \*\*,  $P < 0.01$ . C and D, SW1783 cells transfected with PCDH8 siRNA or with control siRNA were subjected to Transwell migration (C) and invasion (D) assays. Scale bars, 100  $\mu$ m. Data are presented as mean  $\pm$  SD. \*\*\*,  $P < 0.001$ . E, U87 cells transfected with miR-182-5p inhibitor alone or in combination with PCDH8 siRNA and their proliferation were analyzed by the MTT assay. Data are presented as mean  $\pm$  SD. \*\*\*,  $P < 0.001$ ; NS, nonsignificant. F and G, U87 cells transfected with miR-182-5p inhibitor alone or in combination with PCDH8 siRNA were subjected to Transwell migration (F) and invasion (G) assays. Scale bars, 100  $\mu$ m. Data are presented as mean  $\pm$  SD. \*\*\*,  $P < 0.001$ ; NS, nonsignificant.

apoptosis of U87 cells (Supplementary Fig. S3C). These results, in combination with the results in Figs. 2 and 4 showing that miR-182-5p as well as PCDH8 play roles in cell proliferation,

suggest that suppression of STAT3 inhibition-induced apoptosis by miR-182-5p mimics or PCDH8 siRNA is likely caused by increased cell proliferation.

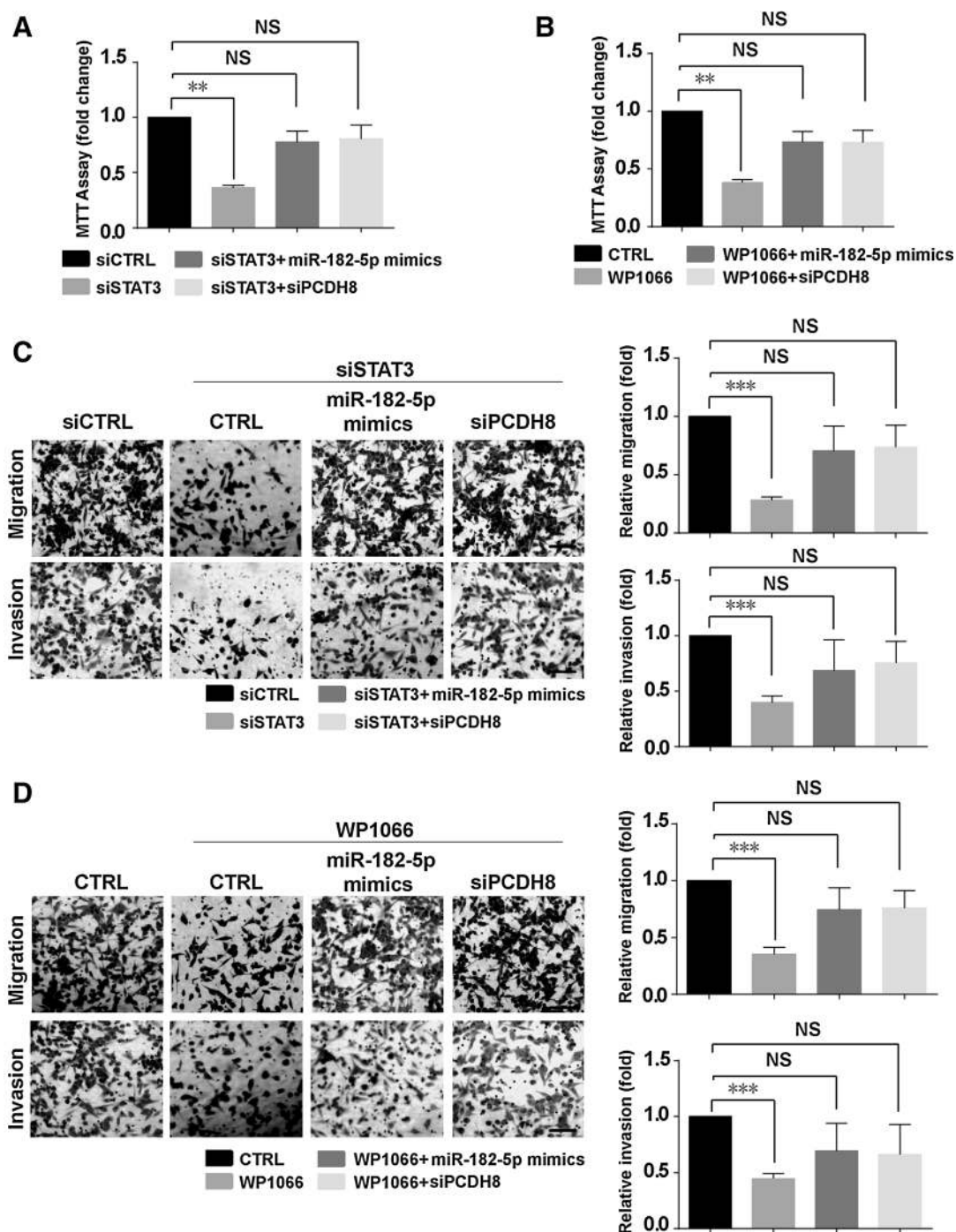


**Figure 5.** miR-182-5p/PCDH8 is essential for STAT3-mediated glioma cell growth, migration, and invasion. A, U87 cells transfected with STAT3 siRNA or with control siRNA alone or in combination with miR-182-5p mimics or PCDH8 siRNA and their proliferation were analyzed by the MTT assay. \*\*,  $P < 0.01$ . B, U87 cells treated with WP1066 alone or in combination with miR-182-5p mimics or PCDH8 siRNA and their proliferation were analyzed by the MTT assay. \*\*,  $P < 0.01$ . C, U87 cells transfected with STAT3 siRNA or with control siRNA alone or in combination with miR-182-5p mimics or PCDH8 siRNA were subjected to Transwell migration and invasion assays. Scale bars, 100  $\mu\text{m}$ . Data are presented as mean  $\pm$  SD. \*\*\*,  $P < 0.001$ ; NS, nonsignificant. D, U87 cells treated with WP1066 alone or in combination with miR-182-5p mimics or PCDH8 siRNA were subjected to Transwell migration and invasion assays. Scale bars, 100  $\mu\text{m}$ . Data are presented as mean  $\pm$  SD. \*\*\*,  $P < 0.001$ ; NS, nonsignificant.

Next, we examined the role of STAT3–miR-182-5p–PCDH8 pathway in cell migration and invasion. We found that migration and invasion of U87 cells were notably blocked after

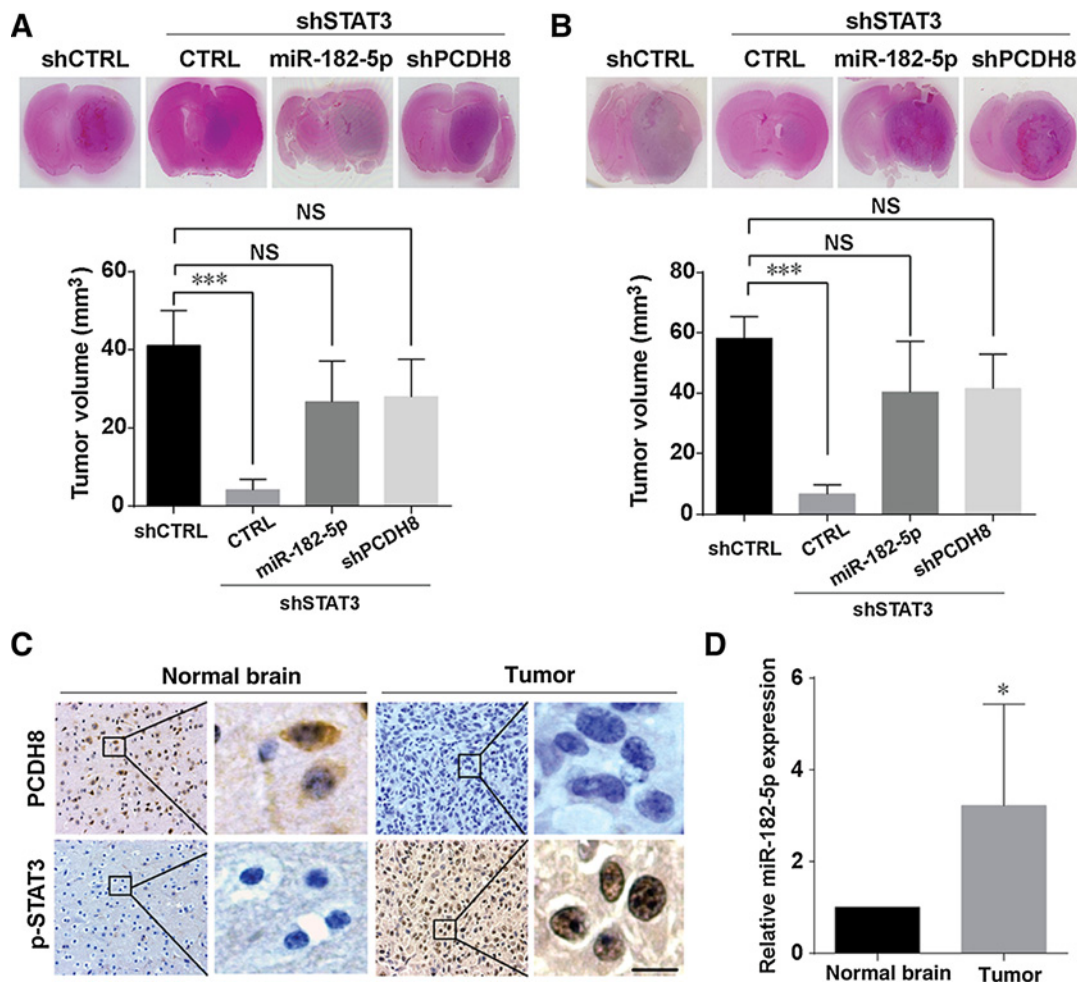
STAT3 knockdown (Fig. 5C) and after WP1066 treatment (Fig. 5D). However, miR-182-5p mimics or PCDH8 siRNA transfection, respectively, rescued these inhibition effects on



migration and invasion (Fig. 5C and D). Moreover, cell-cell adhesion in HFU251 cells was significantly increased by STAT3 knockdown (Supplementary Fig. S3D). When miR-182-5p mimics or PCDH8 siRNA was transfected into the STAT3-inhibited HFU251 cells, the cell-cell adhesion was inhibited (Supplementary Fig. S3D). However, cell-matrix adhesion in U87 and HFU251 cells was not significantly affected by STAT3 knockdown, and miR-182-5p mimics or PCDH8 siRNA also did not change cell-matrix adhesion in the STAT3-inhibited U87 and HFU251 cells (Supplementary Fig. S3E). Thus, the effect of STAT3-miR-182-5p-PCDH8 pathway in cell migration and invasion is likely due, at least in part, to the role of the pathway in cell-cell adhesion. Collectively, the above results suggest that the miR-182-5p-PCDH8 axis is critical for STAT3-induced glioma cell growth, migration, and invasion.

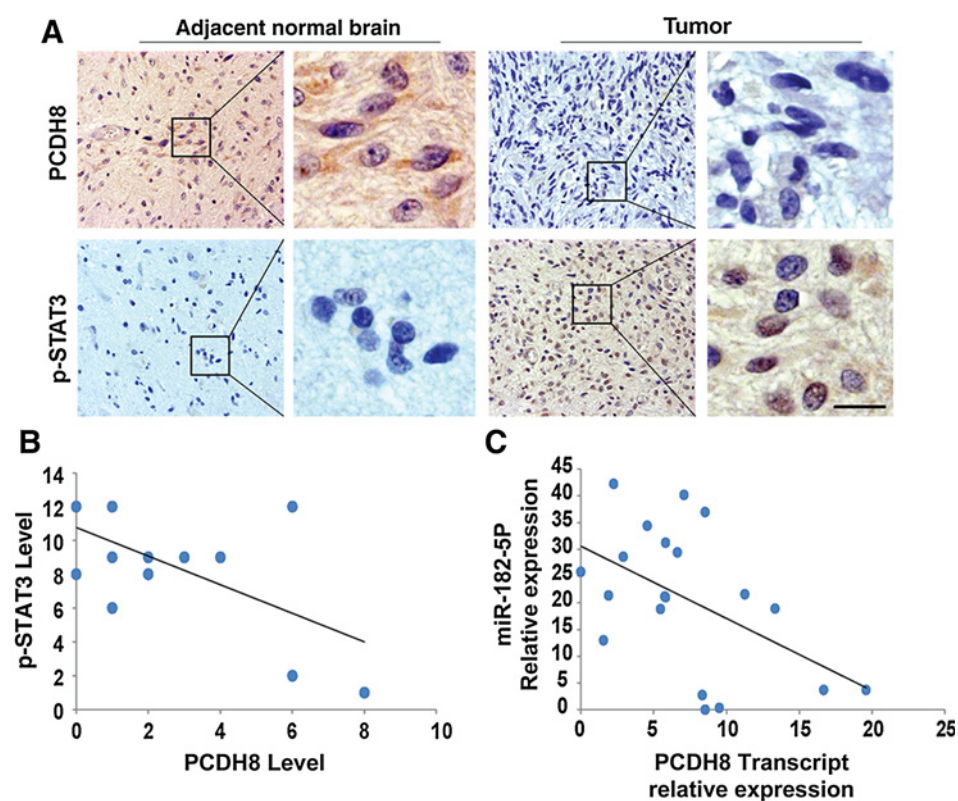
**STAT3-miR-182-5p-PCDH8 pathway promotes tumor growth**

The relevance of our *in vitro* findings was next confirmed *in vivo* by intracranial injection of U87 cells into athymic nude mice. U87 shControl cells did show detectable tumor formation within 4 weeks after injection. In contrast, depleting U87 cells of STAT3 significantly suppressed tumor formation, which was abrogated by miR-182-5p overexpression or knockdown of PCDH8 (Fig. 6A). Similar effects were also observed in HFU251 stable cells (Fig. 6B). We then used IHC staining to evaluate the expression levels of p-STAT3 and PCDH8 in normal brain tissues and in brain tumors produced by U87 cells in nude mice. The expression of PCDH8 was higher in normal brain tissues than in tumor tissues, whereas p-STAT3 expression in the nucleus was higher in tumor tissues (Fig. 6C). Moreover, the expression level of miR-182-5p was significantly higher in



**Figure 6.** STAT3-miR-182-5p-PCDH8 pathway promotes tumor growth. U87 (A) or HFU251 (B) cells with or without depleted STAT3 alone or in combination with miR-182-5p overexpression or PCDH8 knockdown were intracranially injected into athymic nude mice. After 4 weeks, the mice were euthanized, and tumor growth was examined. Top, H&E-stained coronal brain sections show representative tumor xenografts. Bottom, tumor volumes were measured by using length (a) and width (b) and were calculated by using the equation:  $V = ab^2/2$ . Data represent the results of 5 mice per group of two independent experiments. Error bars  $\pm$  SD. Significance was determined by the Mann-Whitney U test. \*\*\*,  $P < 0.001$ . C, brain tumors produced by U87 cells in nude mice were processed and sectioned for immunostaining with specific antibodies against p-STAT3 and PCDH8. Scale bars, 200  $\mu$ m. D, relative ratios of miR-182-5p expression in 5 mice brain tumor tissues compared with 5 normal brain tissues. \*,  $P < 0.05$ .

Downloaded from <http://aacrjournals.org/cancerres/article-pdf/76/14/4293/2731802/4293.pdf> by guest on 25 August 2022

**Figure 7.**

Levels of PCDH8 inversely correlate with the p-STAT3 or miR-182-5p levels. A, IHC staining with p-STAT3 and PCDH8 antibodies was carried out on 20 human glioblastoma specimens. Two representative photographs including the adjacent normal brain tissues and tumor are shown. Scale bars, 200 μm. B, semiquantitative scoring was carried out ( $r = -0.607$ ,  $P < 0.01$ , Pearson correlation coefficient) with all 20 tumors. Note that some of the dots on the graphs represent more than one specimen (i.e., some scores overlapped). C, correlation between miR-182-5p and PCDH8 transcript determined by quantitative real-time RT-PCR in 20 human glioblastoma specimens. Semiquantitative scoring was carried out ( $r = -0.614$ ,  $P < 0.01$ , Pearson correlation coefficient).

tumor tissues than in normal brain tissues by quantitative real-time RT-PCR analysis (Fig. 6D). Together, these findings suggest that the STAT3-miR-182-5p-PCDH8 pathway promotes tumor progression *in vivo*.

#### Levels of PCDH8 inversely correlate with activated STAT3 or miR-182-5p levels

To determine whether our findings have clinical relevance, we examined p-STAT3 and PCDH8 expression levels in serial sections of 20 human primary glioblastoma specimens by IHC analyses. The expression level of PCDH8 in the tumors was significantly lower than that in adjacent normal brain tissues; however, the level of p-STAT3 in tumors was high (Fig. 7A). We further found in tumors that levels of p-STAT3 inversely correlated with levels of PCDH8 expression (Fig. 7B). Quantification of staining showed that this correlation was statistically significant among the 20 specimens ( $r = -0.607$ ;  $P < 0.01$ ; Fig. 7B). Moreover, there was a statistically significant correlation between miR-182-5p levels and PCDH8 transcript levels by quantitative real-time RT-PCR analysis ( $r = -0.614$ ;  $P < 0.01$ ; Fig. 7C). These results further support a critical role for the STAT3-miR-182-5p-PCDH8 pathway promoting tumor progression in human glioblastoma.

## Discussion

It is well-known that miRNAs are critical for the development of the malignant phenotype of glioma cells (27, 28). miR-182-5p is emerging as an important regulator of various physiologic and pathologic processes. miR-182-5p has also been reported to be an oncogene in many types of cancers (14–19, 29–31). In this study, we showed that miR-182-5p

promoted glioma cell growth, migration, and invasion. More importantly, the clinical relevance of miR-182-5p was confirmed in human glioblastoma samples. Therefore, these results firmly established miR-182-5p as a functional mediator of glioma tumorigenesis.

The molecular mechanisms of miR-182-5p regulation in cancer are unclear. STAT3-induced transcription of protein-coding genes has been extensively studied in human cancers; however, the role of STAT3 in the transcription of non-protein-coding genes, such as miRNAs, is less explored. Recent results indicated that the STAT3 transcription factor plays an important role in miRNA expression. For example, STAT3 activated by IL6 directly represses the miR-34a gene, which was shown to be necessary for invasion and metastasis of human colorectal cancer cells and was related to nodal and distant metastasis in patients (32). Furthermore, STAT3-mediated activation of miRNA-23a has been shown to decrease glucose production by directly targeting PGC-1 $\alpha$  and G6PC in hepatocellular carcinoma, thereby facilitating liver tumorigenesis (33). STAT3-activated miR-21 and miR-181b-1 are also required for sphingosine-1-phosphate lyase downregulation that promotes colon carcinogenesis (34). These data cumulatively suggest that STAT3 and miRNAs play a critical role in human cancers. In this study, we provided strong evidence that the activation of miR-182-5p induced by STAT3 activation is important for glioma cell growth, migration, and invasion. We found that STAT3 directly binds two sites in miR-182-5p promoter regions and is required for transcriptional induction of miR-182-5p. In contrast, STAT3 activation by EGF treatment resulted in the upregulation of miR-182-5p. Conversely, inhibition of STAT3 by siRNA or WP1066 strongly reduced miR-182-5p expression levels, suggesting that STAT3 and miR-182-5p are required for

glioma cell growth, migration, and invasion. This study further confirmed that STAT3 acts as a key molecule in the regulation of miRNA in human glioma. Moreover, the results of our study are consistent with the finding in a previous reporter that miR-182 could be a valuable predictor of poor prognosis for patients with glioma (14). Interestingly, another previous study reported that elevated miR-182 levels in proneural subtype glioblastoma tumors negatively correlate with Bcl2L12 levels, and miR-182 increased the apoptosis induced by pan-kinase inhibitor staurosporine in glioblastoma cells through down-regulation of Bcl2L12 (35). It has been shown that activated STAT3 protect tumor cells from apoptosis by upregulating the transcription of Bcl2 family genes such as Bcl-2, Bcl-xL and Mcl-1 (36). Thus, it is possible that in STAT3-activated tumor cells, the effect of miR-182-Bcl2L12 axis on apoptosis is counteracted by the effects of Bcl-2, Bcl-xL, and Mcl-1, whereas miR-182-PCDH8 axis-induced cell growth could further enhance the antiapoptotic effects of Bcl-2, Bcl-xL, and Mcl-1.

PCDH8, a member of the cadherin family, has been shown to be a tumor suppressor involved in tumorigenesis. PCDH8 inhibits oncogenesis in epithelial human cancers by suppressing tumor cell proliferation and inhibiting cell migration (26). The PCDH8 gene promoter is frequently methylated in renal cell carcinoma (~58%), which suggests that it could act as a tumor suppressor or that its tumor suppressor activity is downmodulated in the methylated state (37, 38). Moreover, several studies report that the epigenetic inactivation of PCDH8 by promoter methylation is associated with the loss of its tumor-suppressive function in human nasopharyngeal carcinoma (39), gastric cancer (40), bladder cancer (41), and prostate cancer (42). However, the status of PCDH8 expression in gliomas is unknown. In this study, we found that PCDH8 expression was significantly downregulated in mouse or human brain tumor tissue as compared with normal brain tissue. We also observed a significant negative correlation between p-STAT3 and the PCDH8 protein in human glioblastoma. Moreover, PCDH8 expression was significantly increased by miR-182-5p inhibitor. These findings indicate that the main mechanism in the reduction of PCDH8 protein is miRNA regulation at the posttranscriptional level. Certainly other miRNAs can target PCDH8 such as miR-429, which has been shown to be a regulator of the epithelial-to-mesenchymal tran-

sitional during embryo implantation (43). miR-429 has been shown to inhibit glioma invasion through suppression of a big MAPK (44); however, the link between miR-429 and STAT3 is unknown.

In summary, STAT3 activation induces miR-182-5p to repress PCDH8 expression, leading to glioma cell growth, migration, and invasion. Our results reveal the STAT3-miR-182-5p-PCDH8 axis as potential targets for the development of new therapeutic agents for human glioma.

### Disclosure of Potential Conflicts of Interest

No potential conflicts of interest were disclosed.

### Authors' Contributions

**Conception and design:** J. Xue, A. Zhou, S. Huang

**Development of methodology:** J. Xue, A. Zhou, Y. Wu, K. Lin, S. Huang

**Acquisition of data (provided animals, acquired and managed patients, provided facilities, etc.):** J. Xue, Y. Wu, S.-A. Morris, R. Verhaak, G.N. Fuller, K. Xie, S. Huang

**Analysis and interpretation of data (e.g., statistical analysis, biostatistics, computational analysis):** J. Xue, Y. Wu, S.-A. Morris, K. Lin, S.B. Amin, K. Xie, A.B. Heimberger, S. Huang

**Writing, review, and/or revision of the manuscript:** J. Xue, A. Zhou, S.-A. Morris, G.N. Fuller, A.B. Heimberger, S. Huang

**Administrative, technical, or material support (i.e., reporting or organizing data, constructing databases):** K. Lin, S. Huang

**Study supervision:** S. Huang

### Acknowledgments

The authors thank Tamara Locke in The University of Texas MD Anderson Cancer Center's Department of Scientific Publications for editing this article.

### Grant Support

This work was supported in part by U.S. National Cancer Institute grants R01CA157933, R01CA182684, P50CA127001, and CA16672 (Cancer Center Support Grant) and the National Natural Science Foundation of China (81502184 to J. Xue).

The costs of publication of this article were defrayed in part by the payment of page charges. This article must therefore be hereby marked *advertisement* in accordance with 18 U.S.C. Section 1734 solely to indicate this fact.

Received November 10, 2015; revised March 30, 2016; accepted April 23, 2016; published OnlineFirst May 31, 2016.

### References

1. Sturm D, Bender S, Jones DT, Lichter P, Grill J, Becher O, et al. Paediatric and adult glioblastoma: multifactorial (epi) genomic culprits emerge. *Nat Rev Cancer* 2014;14:92-107.
2. Claes A, Idema AJ, Wesseling P. Diffuse glioma growth: a guerilla war. *Acta Neuropathol* 2007;114:443-58.
3. Bromberg J, Darnell JE Jr. The role of STATs in transcriptional control and their impact on cellular function. *Oncogene* 2000;19:2468-73.
4. Yu H, Jove R. The STATs of cancer-new molecular targets come of age. *Nat Rev Cancer* 2004; 4:97-105.
5. Doucette TA, Kong LY, Yang Y, Ferguson SD, Yang J, Wei J, et al. Signal transducer and activator of transcription 3 promotes angiogenesis and drives malignant progression in glioma. *Neuro Oncol* 2012;14:1136-45.
6. Vultur A, Cao J, Arulanandam R, Turkson J, Jove R, Greer P, et al. Cell-to-cell adhesion modulates Stat3 activity in normal and breast carcinoma cells. *Oncogene* 2004;23:2600-16.
7. Yu H, Lee H, Herrmann A, Buettner R, Jove R. Revisiting STAT3 signaling in cancer: new and unexpected biological functions. *Nat Rev Cancer* 2014;14:736-46.
8. Gong AH, Wei P, Zhang S, Yao J, Yuan Y, Zhou AD, et al. FoxM1 drives a feed-forward STAT3-activation signaling loop that promotes the self-renewal and tumorigenicity of glioblastoma stem-like cells. *Cancer Res* 2015;75:2337-48.
9. Wei J, Wang F, Kong LY, Xu S, Doucette T, Ferguson SD, et al. miR-124 inhibits STAT3 signaling to enhance T cell-mediated immune clearance of glioma. *Cancer Res* 2013;73:3913-26.
10. Abou-Ghazal M, Yang DS, Qiao W, Reina-Ortiz C, Wei J, Kong LY, et al. The incidence, correlation with tumor-infiltrating inflammation, and prognosis of phosphorylated STAT3 expression in human gliomas. *Clin Cancer Res* 2008;14:8228-35.
11. Lin S, Gregory RI. MicroRNA biogenesis pathways in cancer. *Nat Rev Cancer* 2015;15:321-33.
12. Zimmerman AL, Wu S. MicroRNAs, cancer and cancer stem cells. *Cancer Lett* 2011;300:10-9.
13. Shen J, Hung MC. Signaling-mediated regulation of MicroRNA processing. *Cancer Res* 2015;75:783-91.
14. Song L, Liu L, Wu Z, Li Y, Ying Z, Lin C, et al. TGF- $\beta$  induces miR-182 to sustain NF- $\kappa$ B activation in glioma subsets. *J Clin Invest* 2012;122:3563-78.

15. Zhu W, Liu X, He J, Chen D, Hunag Y, Zhang YK. Overexpression of members of the microRNA-183 family is a risk factor for lung cancer: a case control study. *BMC Cancer* 2011;11:393.
16. Lei R, Tang J, Zhuang X, Deng R, Li G, Yu J, et al. Suppression of MIM by microRNA-182 activates RhoA and promotes breast cancer metastasis. *Oncogene* 2014;33:1287–96.
17. Liu R, Li J, Teng Z, Zhang Z, Xu Y. Overexpressed microRNA-182 promotes proliferation and invasion in prostate cancer PC-3 cells by down-regulating N-myc downstream regulated gene 1 (NDRG1). *PLoS One* 2013;8:e68982.
18. Wang J, Li J, Shen J, Wang C, Yang L, Zhang X. MicroRNA-182 down-regulates metastasis suppressor 1 and contributes to metastasis of hepatocellular carcinoma. *BMC Cancer* 2012;12:227.
19. Perilli L, Vicentini C, Agostini M, Pizzini S, Pizzi M, D'Angelo E, et al. Circulating miR-182 is a biomarker of colorectal adenocarcinoma progression. *Oncotarget* 2014;5:6611–9.
20. Liu M, Dai B, Kang SH, Ban K, Huang FJ, Lang FF, et al. FoxM1B is overexpressed in human glioblastomas and critically regulates the tumorigenicity of glioma cells. *Cancer Res* 2006;66:3593–602.
21. Xue J, Lin X, Chiu WT, Chen YH, Yu C, Liu M, et al. Sustained activation of SMAD3/SMAD4 by FOXM1 promotes TGF- $\beta$ -dependent cancer metastasis. *J Clin Invest* 2014;124:564–79.
22. Xue J, Chen Y, Wu Y, Wang Z, Zhou A, Zhang S, et al. Tumour suppressor TRIM33 targets nuclear  $\beta$ -catenin degradation. *Nat Commun* 2015;6: 6156.
23. Lee HT, Xue J, Chou PC, Zhou A, Yang P, Conrad CA, et al. Stat3 orchestrates interaction between endothelial and tumor cells and inhibition of Stat3 suppresses brain metastasis of breast cancer cells. *Oncotarget* 2015;6: 10016–29.
24. Hussain SF, Kong LY, Jordan J, Conrad C, Madden T, Fokt I, et al. A novel small molecule inhibitor of signal transducers and activators of transcription 3 reverses immune tolerance in malignant glioma patients. *Cancer Res* 2007;67:9630–6.
25. Iwamaru A, Szymanski S, Iwado E, Aoki H, Yokoyama T, Fokt I, et al. A novel inhibitor of the STAT3 pathway induces apoptosis in malignant glioma cells both *in vitro* and *in vivo*. *Oncogene* 2007;26:2435–44.
26. Yu JS, Koujak S, Nagase S, Li CM, Su T, Wang X, et al. PCDH8, the human homolog of PAPC, is a candidate tumor suppressor of breast cancer. *Oncogene* 2008;27:4657–65.
27. Kim J, Zhang Y, Skalski M, Hayes J, Kefas B, Schiff D, et al. microRNA-148a is a prognostic oncomiR that targets MIG6 and BIM to regulate EGFR and apoptosis in glioblastoma. *Cancer Res* 2014;74:1541–53.
28. Li Y, Guessous F, Zhang Y, Dipierro C, Kefas B, Johnson E, et al. MicroRNA-34a inhibits glioblastoma growth by targeting multiple oncogenes. *Cancer Res* 2009;69:7569–76.
29. Segura MF, Hanniford D, Menendez S, Reavie L, Zou X, Alvarez-Diaz S, et al. Aberrant miR-182 expression promotes melanoma metastasis by repressing FOXO3 and microphthalmia-associated transcription factor. *Proc Natl Acad Sci* 2009;106:1814–9.
30. Guttilla IK, White BA. Coordinate regulation of FOXO1 by miR-27a, miR-96, and miR-182 in breast cancer cells. *J Biol Chem* 2009;284:23204–16.
31. Mihelich BL, Khrantsova EA, Arva N, Vaishnav A, Johnson DN, Giangreco AA, et al. miR-183-96-182 cluster is overexpressed in prostate tissue and regulates zinc homeostasis in prostate cells. *J Biol Chem* 2011; 286:44503–11.
32. Rokavec M, Öner MG, Li H, Jackstadt R, Jiang L, Lodygin D, et al. IL-6R/STAT3/miR-34a feedback loop promotes EMT-mediated colorectal cancer invasion and metastasis. *J Clin Invest* 2014;124:1853–67.
33. Wang B, Hsu SH, Frankel W, Ghoshal K, Jacob ST. Stat3-mediated activation of microRNA-23a suppresses gluconeogenesis in hepatocellular carcinoma by down-regulating glucose-6-phosphatase and peroxisome proliferator-activated receptor gamma, coactivator 1 alpha. *Hepatology* 2012;56:186–97.
34. Degagné E, Pandurangan A, Bandhuvula P, Kumar A, Eltanawy A, Zhang M, et al. Sphingosine-1-phosphate lyase downregulation promotes colon carcinogenesis through STAT3-activated microRNAs. *J Clin Invest* 2014; 124:5368–84.
35. Kouri FM, Hurley LA, Daniel WL, Day ES, Hua Y, Hao L, et al. miR-182 integrates apoptosis, growth, and differentiation programs in glioblastoma. *Genes Dev* 2015;29:732–45.
36. Huang S. Regulation of metastases by signal transducer and activator of transcription 3 signaling pathway: clinical implications. *Clin Cancer Res* 2007;13:1362–6.
37. Leshchenko VV, Kuo PY, Shakhovich R, Yang DT, Gellen T, Petrich A, et al. Genomewide DNA methylation analysis reveals novel targets for drug development in mantle cell lymphoma. *Blood* 2010;116:1025–34.
38. Morris MR, Ricketts CJ, Gentle D, McRonald F, Carli N, Khalili H, et al. Genome-wide methylation analysis identifies epigenetically inactivated candidate tumour suppressor genes in renal cell carcinoma. *Oncogene* 2011;30:1390–401.
39. Zhang D, Zhao W, Liao X, Bi T, Li H, Che X. Frequent silencing of protocadherin 8 by promoter methylation, a candidate tumor suppressor for human gastric cancer. *Oncol Rep* 2012;28:1785–91.
40. He D, Zeng Q, Ren G, Xiang T, Qian Y, Hu Q, et al. Protocadherin8 is a functional tumor suppressor frequently inactivated by promoter methylation in nasopharyngeal carcinoma. *Eur J Cancer Prev* 2012;21: 569–75.
41. Lin YL, Ma JH, Luo XL, Guan TY, Li ZG. Clinical significance of protocadherin-8 (PCDH8) promoter methylation in bladder cancer. *J Exp Clin Cancer Res* 2014;33:68.
42. Niu WB, Gui SL, Lin YL, Fu XL, Ma JG, Li WP. Promoter methylation of protocadherin8 is an independent prognostic factor for biochemical recurrence of early-stage prostate cancer. *Med Sci Monit* 2014; 20:2584–9.
43. Li Z, Gou J, Jia J, Zhao X. MicroRNA-429 functions as a regulator of epithelial-mesenchymal transition by targeting Pcdh8 during murine embryo implantation. *Hum Reprod* 2015;30:507–18.
44. Chen W, Zhang B, Guo W, Gao L, Shi L, Li H, et al. miR-429 inhibits glioma invasion through BMK1 suppression. *J Neurooncol* 2015;125:43–54.